

A Comparative Investigation on Electrochemical Impedance Studies and Surface Characterization Techniques in Corrosion Protection of Copper Using Thiol, Imidazole and Aminoacid Self-Assembled Monolayers in Neutral Media.

A. Rajalakshmi Devi

Assistant Professor, Department of Chemistry, V.S.B. Engineering College, Karur-639 111, Tamil Nadu, India

Abstract

As corrosion protection of copper is also efficiently done using, Self-Assembled Monolayers using thiols, imidazoles and aminoacids, the present work is done as a comparative study of EIS and surface characterization techniques of thiols, imidazoles and aminoacids in corrosion protection of copper using SAMs in neutral media.

Key words SAMs, EIS, 5-methyl-1,3,4-thiadiazole-2-thiol, 2-methyl-5-nitroimidazole, Azepane-1-carbodithioic acid, corrosion protection

1. INTRODUCTION

The corrosion of copper and other metals occur usually when it is exposed to air. Copper is also exclusively used for piping and delivery of water for marine industries, which mainly contains sodium chloride. The high concentration of chloride ions severely leads to corrosion of copper. Various strategies have been applied to address the growing need for inhibition of copper corrosion. One of the most efficient approaches for protecting copper against aggressive attack is the formation of ultrathin films using SAMs

2. EXPERIMENTAL PROCEDURE

2.1. Chemical and Method

99.99% AR grade pure chemicals 5-methyl-1,3,4-thiadiazole-2-thiol, 2-methyl-5-nitroimidazole are obtained from Sigma-Aldrich and synthesised Azepane-1-carbo-dithioic acid (using Diethyl imine and Carbon-di-sulphide in presence of sodium hydroxide under ice cold condition are used). Absolute ethanol (GR) grade is used as the solvent for preparing thiol and imidazole solutions of required concentrations. And triple distilled water is used as the solvent for preparing aminoacid solution of various concentrations. Sodium chloride of Merck analytical grade reagent and triple distilled water are used for preparing electrolyte solution.

2.2. Electrode Preparation

A copper rod of 99.99% purity with cross-sectional area of 1cm^2 embedded in epoxy resin leaving its sq-

quare cross-section is used for electrochemical measurements. The copper electrode to be used is cleaned to mirror finish using various grade emery sheets and degreased with acetone. A dense and stable SAMs can be formed with an immersion time more than 20 hrs with the lowest concentration of the inhibitor used[1,2]. So, for the present study an immersion period of 24 hr and a concentration of 5 to 20 ppm of the inhibitor is used.

3. Results and Discussion

Electrochemical Impedance Studies

This is used to characterise the properties of SAMs [3-7]. This study is based on the measurement of the response to an alternating potential of small amplitude. Nquist plots of bare copper and SAMs covered copper electrodes are obtained in 300 ppm aqueous sodium chloride solution after half an hour equilibration as the open-circuit potentials of the electrodes become steady. Impedance parameters for the bare and SAMs covered copper electrodes are obtained using three different equivalent circuit models [8, 9] shown below

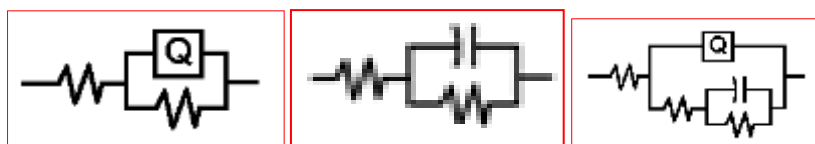


Fig. 3.1.a.

Fig. 3.1.b.

Fig. 3.1.c.

Figures 3.1.a, b & c - Equivalent circuits

Bode plots also provide the much needed information than the Nquist plots. The phase angle is at the maximum of 70° , 78° and 76° for thiol, imidazole and aminoacids SAMs covered copper than bare copper. The Nquist plots for bare and thiol, imidazole and aminoacids SAMs covered copper in sodium chloride at different concentrations at a constant immersion period of half an hour, at a temperature of 30°C and for various immersion periods in the neutral media are shown in **Figures 3.2 to 3.5**. The impedance data for bare copper and SAMs covered copper are shown in **table 3.1 to 3.3**. For e.g., The R_{ct} value for bare copper in 300 ppm sodium chloride solution is $2.56 \text{ K}\Omega \text{ cm}^2$, which have increased enormously to $55.192 \text{ K}\Omega \text{ cm}^2$, $34.113 \text{ K}\Omega \text{ cm}^2$ and $28.45 \text{ K}\Omega \text{ cm}^2$ for copper covered with thiol, imidazole and amino acids SAMs for the same environment. The CPE value at the copper interface is found to decrease from $0.044 \mu\text{F cm}^2$ to $0.000098 \mu\text{F cm}^2$, $0.00026 \mu\text{F cm}^2$ and $0.00037 \mu\text{F cm}^2$ for bare copper to thiol, imidazole and amino acids SAMs covered copper. This is because the water molecules in the electrical double layer are replaced to a very large extent by the organic molecules having a very low dielectric constant [10]. The value of n has increased from bare copper to SAMs covered copper and as a result, the copper surface has become smoother due to the formation of dense, non-porous monolayer of 5-methyl-1,3,4-thiadiazole-2-thiol, 2-methyl-5-nitimidazole and Azepane-1-carbodithioic acid Self-Assembled Monolayers respectively. When the value of n drops to unity slowly, the behaviour of SAMs formed tend to be an ideal capacitor [11].

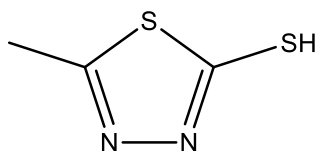
The changes in the double layer capacitance and interfacial capacitance have been found to be correlated with SAMs formation. In addition, the polarization resistance, which corresponds to the charge transfer resistance of the monolayer, increases with the increase in the SAMs coverage. Since the double layer capacitance is larger than the capacitance of SAMs due to thiol, imidazole and aminoacid monolayer, the high frequency EIS data is modelled with a Randle's circuit modified with a constant phase element

(CPE) in place of the capacitor as shown in **Figures 4.2.4. a to c**. The very same is observed, with varying immersion periods and with varying sodium chloride concentration irrespective of thiol, imidazole and aminoacid monolayers. The impedance of CPE depends on the frequency via the equation,

$$Z_{CPE} = 1/C (j\omega)^n$$

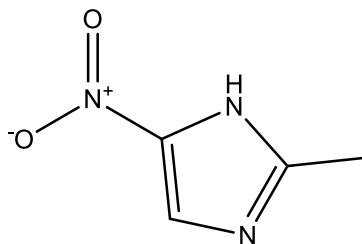
Where, C- the capacitance.

The studies of Nahir and Bowden [12] have shown that electrons can penetrate SAMs even though they are defect free and more-over SAMs are found to contain molecule sized defects [13-16]. Zamborini and Crooks [13] have proposed a corrosion reaction model for the electrode covered by SAMs with defects. In this model, the corrosive ions, such as halide ions, can penetrate through SAMs through defects and react with metal substrate, giving rise to the expansion of the defective sites and leading to further destruction of SAMs. But hydrocarbons containing nitrogen and sulphur within the SAMs can partially heal the defects. Hence, in such case, 5-methyl-1,3,4-thiadiazole-2-thiol $\{C_3H_4N_2S_2\}$



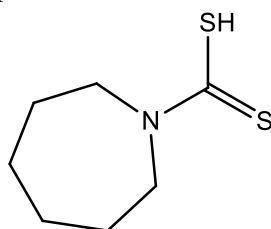
5-Methyl-1,3,4-thiadiazole 2-thiol

containing two nitrogen and two sulphur atoms, 2-methyl-5-nitroimidazole $\{C_4H_4N_3O_2\}$



2-Methyl-5-nitroimidazole

containing three nitrogen atoms and Azepane-1-carbo dithioic acid $\{C_7H_{13}N_2S_2\}$



containing one nitrogen and two sulphur atoms, bond tightly to the metal surface thus forming a very thick monolayer that prevents the diffusion of corroding chemicals and ions and offers a great protection for copper from being corroded. And the inhibition efficiency is calculated using the formula, I.E. = $(R_t^1 - R_t) \times 100 / R_t^1$

Where, R_t^1 the resistance of SAMs covered copper and R_t the resistance of bare copper respectively. And the results found a very good correlation with polarization and weight-loss studies.

Thus, all the observations in the impedance studies indicate that there is the formation of non-porous, highly protective film (SAMs) on the metal surface, which effectively protect the metal from corrosion even in aggressive environment like sodium chloride of very lowest concentration where pitting corrosion is possible.

Conc. (ppm)	R_{ct} ($K\Omega\text{ cm}^2$)	Cdl ($\mu F\text{ cm}^2$)	n	IE (%)
Bare copper	2.56	0.044	0.35	-
5 Thiol	55.192	0.000098	0.92	95
Imidazole	21.522	0.00066	0.85	88
Aminoacid	6.32	0.0076	0.52	59
10 Thiol	7.754	0.0034	0.56	67
Imidazole	34.113	0.00026	0.90	92
Aminoacid	8.43	0.0043	0.61	70
15 Thiol	13.576	0.0016	0.76	81
Imidazole	30.02	0.00034	0.89	91
Aminoacid	10.11	0.0029	0.64	75
20 Thiol	12.841	0.0018	0.75	80
Imidazole	28.522	0.020	0.88	91
Aminoacid	28.45	0.00037	0.87	91

Table 3.1. Impedance parameters of bare and SAMs covered copper in aq. 300 ppm sodium chloride solution at different concentrations of the inhibitor

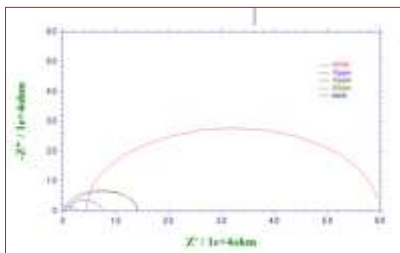


Fig. 3.2.a.

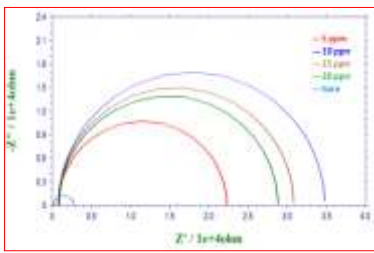


Fig. 3.2.b.

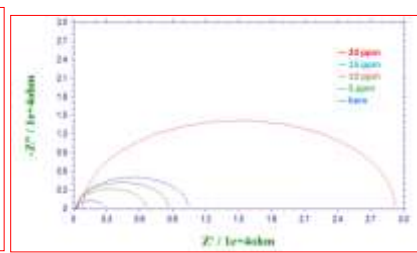


Fig. 3.2.c.

Figures 3.2.a. to c. Niquist plots of bare and SAMs covered copper (thiol, imidazole & aminoacid) in aq. 300 ppm sodium chloride solution

Conc.	R_c ($K\Omega\text{ cm}^2$)	Cdl ($\mu F\text{ cm}^2$)	n	IE (%)
Blank 1 hr	1.36	0.166	0.25	-
Thiol	19.01	0.0014	0.92	93
Imidazole	168.75	0.00004	0.97	99
Aminoacid	40.106	0.00019	0.96	97
Blank 2 hr	0.222	6.264	0.15	-
Thiol	18.54	0.0015	0.96	99
Imidazole	10.158	0.0095	0.96	98
Aminoacid	60.004	0.00008	0.98	99
Blank 4 hr	0.198	7.804	0.15	-
Thiol	26.12	0.00093	0.96	99
Imidazole				
Aminoacid	5.523	0.033	0.95	96

	2.661	0.044	0.90	93
Blank 6hr	0.154	12.867	0.12	-
Thiol	123.89	0.000058	0.97	99
Imidazole	148.14	0.000007	0.98	99
Aminoacid	3.079	0.0327	0.94	95

Table 3.2. Impedance parameters of bare and SAMs covered copper at different immersion periods in aq. 300 ppm chloride

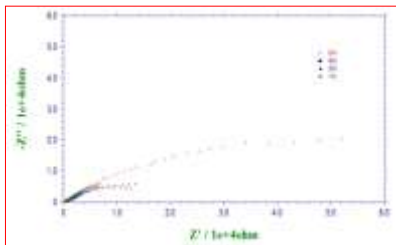


Fig. 3.3.a.

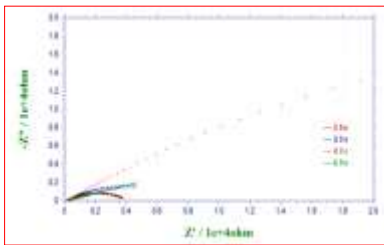


Fig. 3.3.b.

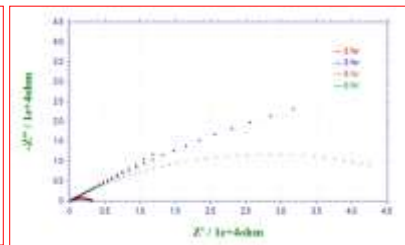


Fig. 3.3.c.

Figures 3.3.a. to c. Nyquist plots of SAMs covered copper (thiol, imidazole & aminoacid) at different immersion periods in aq. 300 ppm chloride

Conc. (ppm)	R _t (KΩ cm ²)	Cdl (μF cm ²)	n	IE (%)
B 100	0.843	0.4183	0.20	-
Thiol	8.23	0.00456	0.85	90
Imidazole	2.002	0.163	0.47	58
Aminoacid	59.008	0.000088	0.97	99
B 150	0.728	0.5496	0.19	-
Thiol	6.112	0.00804	0.80	88
Imidazole	1.252	0.193	0.33	42
Aminoacid	22.787	0.00059	0.95	97
B 200	0.680	0.6423	0.18	-
Thiol	3.443	0.0255	0.75	80
Imidazole	1.109	0.25	0.35	39
Aminoacid	9.945	0.00309	0.89	93
B 250	0.375	2.050	0.16	-
Thiol	2.339	0.00555	0.77	84
Imidazole	4.376	0.0755	0.87	91
Aminoacid	6.481	0.0073	0.92	94
B 300	2.56	0.4	0.35	-
Thiol	55.192	0.000098	0.94	95
Imidazole	34.113	0.00026	0.90	92

Aminoacid	28.45	0.00037	0.87	91
-----------	-------	---------	------	----

Table 3.3. Impedance parameters of bare and SAMs covered copper of 5 ppm inhibitor concentration in different concentration of aq. Sodium chloride solution

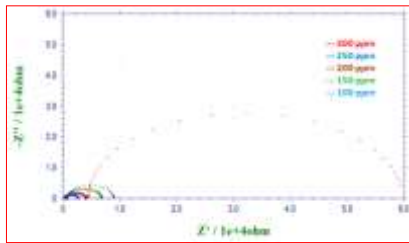


Fig. 3.4.a.

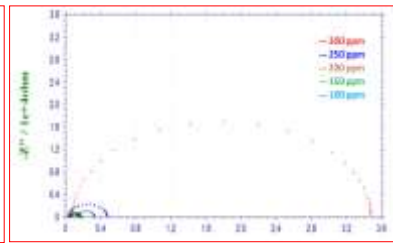


Fig. 3.4.b.

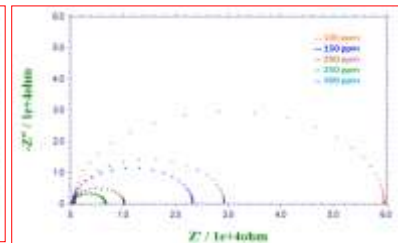


Fig. 3.4.c.

Figures 3.4.a. to c. Nyquist plots of SAMs covered copper (thiol, imidazole & aminoacid) in different concentrations of aq. Sodium chloride solution

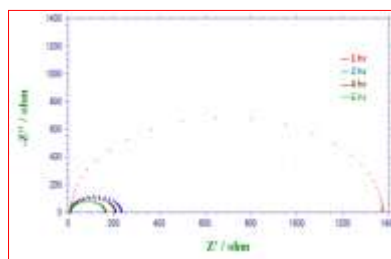


Fig. 3.5.a.

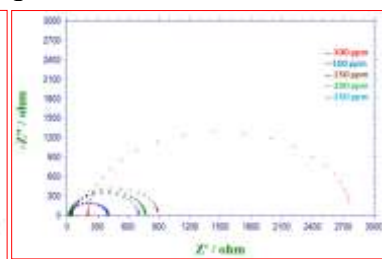


Fig. 3.5.b.

Figures 3.5.a. & b. Nyquist plots of bare copper at a) different immersion periods in aq. 300 ppm chloride b) different concentrations of aq. Sodium chloride solution.

4. AFM (Atomic Force Microscopy) studies

Environment	Ra (µm)	Rms (µm)
Polished Cu metal	0.9504	1.404
Polished Cu metal in 300 ppm Cl-	2.435	2.463
Thiol SAM covered metal surface	2.106	2.279
Imidazole SAM covered metal surface	1.480	1.498
Amino acid SAM covered metal surface	1.834	2.133

Table 4.1. AFM Parameters

Atomic force microscopy (AFM) or scanning force microscopy (SFM) is a very high resolution type of scanning probe and it is considered to be one of the most powerful methods to investigate surface morphology of SAMs on copper surface. It is a powerful technique to investigate the surface morphology at nano- to micro-scale [17]. The thickness in turn the roughness of the Self-assembled monolayer formed on the copper surface can be measured using AFM studies through contact and non-contact modes. For the present work, it is done through contact mode. The topography of the surfaces recorded in 2D and 3D images are examined and surface roughness, root-mean-square roughness (Rms), mean roughness factor (Ra) are determined from the respective images. The more the thickness of the SAMs layer, more will be the corrosion inhibition efficiency. **Table 4.1.** shows various AFM parameters

obtained for SAMs covered copper surfaces. **Figures 4.1.1.a & b** show the AFM images and cross section analysis of polished metal surface, with an Ra value of 0.9504 μm , Rms value of 1.404 μm indicate the absence of SAMs. A severely corroded surface morphology (**Figure 4.2.16.a**) is observed after immersion in 300 ppm aqueous sodium chloride solution, with an increased Ra value of 2.435 μm , Rms value of 2.463 μm indicate the adsorption of chloride ions and the formation of corrosion products. The root-mean-square (RMS) roughness is found to be 2.463 μm , which clearly indicates the roughness of the corroded surface. The microstructure of the surface shows several smaller and larger corrosion product deposits. Whereas **Figures 4.1.3.a to c** indicate the decrease in roughness of the SAMs covered copper surface which shows the dense, uniform adsorption of thiol on the metal surface. The decrease in RMS roughness from 2.463 μm from bare to 2.279 μm for thiol covered SAMs copper and 1.480 μm from polished copper to 1.498 μm for imidzole covered SAMs copper from 1.834 μm from polished copper to 2.133 μm for Aminoacid covered SAMs clearly infer the greater smoothness and homogeneity of the surface film produced by the the thiol, imidazole and the aminoaid and the absence of any corrosion product deposits thus offer a protective layer thereby, forming a great barrier against the attack of aggressive ions from the corrosive environment.

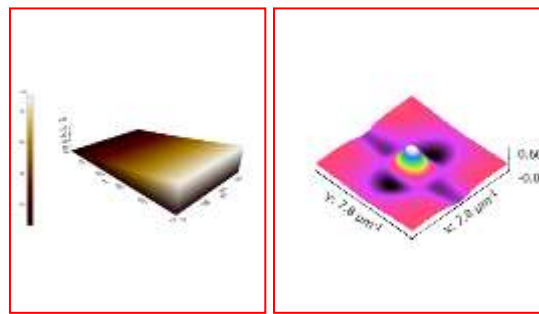


Fig. 4.1.1.a.

Fig. 4.1.1.b.

Figures 4.1.1. a & b refer to the AFM images and cross section analysis of pure copper

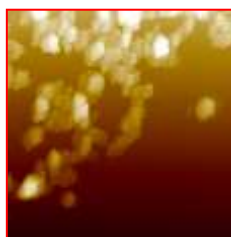


Fig. 4.1.2.a.

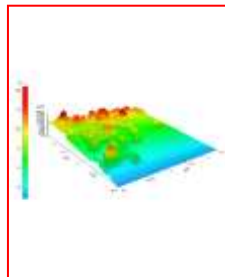


Fig. 4.1.2.b.

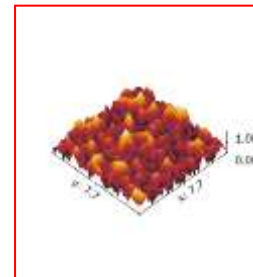


Fig. 4.1.2.c.

Figures 4.1.2.a, b & c refer to the AFM images and cross section analysis of SAMs covered copper specimen

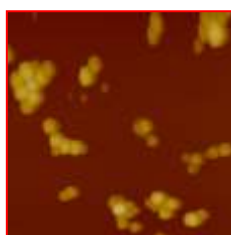


Fig. 4.1.3.a.

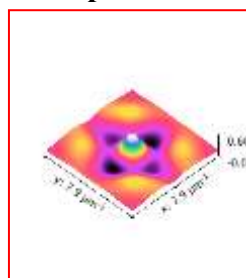


Fig. 4.1.3.b.

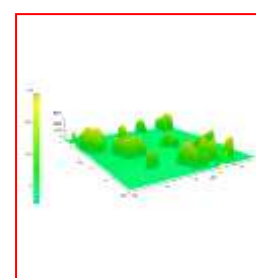


Fig. 4.1.3.c.

Figures 4.1.3. a, b & c refer to the AFM images and cross section analysis of polished copper in 300 ppm sodium chloride solution



Fig. 4.1.4.a.



Fig. 4.1.4.b.

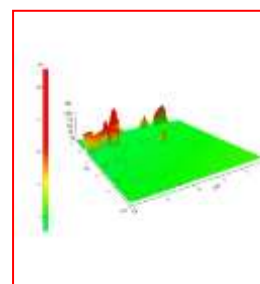


Fig. 4.1.4.c.

Figures 4.1.4.a, b & c refer to the AFM images and cross section analysis of SAMs covered copper specimen

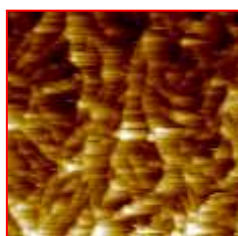


Fig. 4.1.5.a.

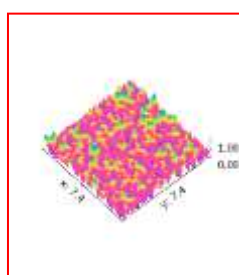


Fig. 4.1.5.b.

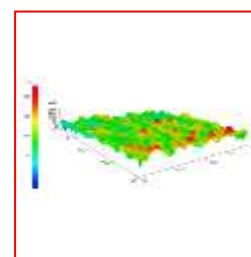


Fig. 4.1.5.c.

Figures. 4.1.5.a, b & c refer to AFM images and cross section analysis of SAMs covered copper

5. XPS (X-ray Photoelectron Spectroscopy) studies

It is a surface sensitive quantitative spectroscopic technique that measures the elemental composition at the parts per thousand range and the electronic state of the element that exists within a material, in the surface modification of the copper plates by chemisorption of self-assembled monolayers through nitrogen, sulphur or oxygen, where the adsorption of Cu, N, S, O take place in different energy levels of 2p and 1s. The origin is the photoelectric effect in which, a highly energetic photon interacts with matter, causing an electron to be moved from an atomic orbital or from a band and to reach the vacuum level.

The XPS survey spectrum of polished copper and the corresponding computer deconvoluted spectra for the peaks due to Cu 2p, C 1s and O 1s electrons are shown in **Fig. 5.1.2.a.** respectively. The Cu 2p_{3/2} at a binding energy of 932.5 eV and is attributed to Cu (I) or metallic copper. Since there appears another Cu 2p_{1/2} peak at 952.5 eV and O 1s peak at 533 eV, it is confirmed that the Cu 2p peak is of Cu (I) species, which is due to the formation of Cu₂O and not of metallic copper. The XPS survey spectrum of bare copper after the immersion in 300 ppm sodium chloride solution for a period of three days is shown in **Fig. 5.1.3.a.** Cu 2p_{3/2}, Cu 2p_{1/2} and O 1s peaks are detected along with the peak of Cl 2p at 200.2 eV. The peaks due to copper and oxygen are similar to those of the peaks obtained for bare copper and the presence of Cl 2p peak of bare copper in NaCl might be due to the formation of CuCl₂ on copper surface and the corresponding deconvolution spectra have been shown in **Fig. 5.1.3.b.**

The XPS survey spectrum of copper covered with SAMs show peaks due to Cu 2p, O 1s, C 1s, N 1s and S 2p and the corresponding computer deconvolution spectra are shown in **Fig. 5.1.1.b.** The Cu 2p_{3/2} peak at 932.5 eV confirms the presence of cuprous copper due to Cu₂S, which shows the cleavage of S-H bond in thiol and sulphur in thiol molecule is involved in complex formation with copper (I) ions and

C 1s peak at 284 eV is due to the presence of carbon atoms in the alkyl chain of methyl thiol. The N 1s peak at 400 eV and S 2p peak at 164 eV show the presence of nitrogen and sulphur. And nitrogen in the third position of thiol can donate the electron pair easily to form a bond with copper. Therefore, the electron density on this nitrogen is reduced and the binding energy is shifted to a higher value of 400 eV from 398 eV [18]. Both nitrogen and sulphur form complex with copper (I) ions through chelation. And the formation of this thin inhibitor film is in agreement with the SEM observations. And the appearance of O 1s peak may be due to the formation of cuprous oxide in the initial stages of SAMs formation.

The XPS survey spectrum of bare copper after the immersion in 300 ppm sodium chloride solution for a period of three days is shown in **Fig. 5.1.4. a**. Cu 2p_{3/2}, Cu 2p_{1/2} and O 1s peaks are detected along with the peak of Cl 2p at 200.2 eV. The peaks due to copper and oxygen are similar to those of the peaks obtained for bare copper, which shows the presence of Cu (I) species and the presence of Cl 2p peak of bare copper in NaCl is due to the formation of CuCl₂ on copper surface and the corresponding deconvolution spectra has been shown in **Fig. 5.1.4.b**. The XPS survey spectrum of copper covered with SAMs show peaks due to Cu 2p, O 1s, C 1s, N 1s and the corresponding computer deconvoluted spectra are shown in **Fig. 5.1.4.a to e**. The Cu 2p_{3/2} peak at 937 eV and Cu 2p_{1/2} peak at 957 eV show the presence of cuprous copper and not of cupric copper as no peak around 940 to 942 eV has appeared. And the absence of satellite peak confirms the absence of cupric copper and C 1s peak at 290 eV is due to the presence of carbon atoms in the alkyl chain. The O 1s peak at 537 eV with the shift of +1 eV shows the presence of oxygen in the imidazole molecule itself. The N 1s peak at 400 eV and 410 eV shows the presence of nitrogen in the first and third position in the imidazole molecule, which can be explained as nitrogen in the third position can donate the electron pair easily to form a bond with copper. Therefore, the electron density on this nitrogen is reduced and the binding energy is shifted to a higher value from 398 eV. Thus the shift in the elemental binding energies of N 1s reveal that the nitrogen atoms present in 2-methyl-5-nitroimidazole are involved in the complex formation with copper through cuprous ions and the results are in agreement with SEM analysis.

The XPS survey spectrum of copper covered with SAMs showed peaks due to Cu 2p, O 1s, C 1s, N 1s and S 2p and the corresponding computer deconvoluted spectra are shown in **Fig. 5.1.5.a. to f**. The Cu 2p_{3/2} peak at 934 eV and another peak at 954 eV with the deviation of +1 eV and +2 eV show the presence of cuprous copper and C 1s peak at 286.64 eV is due to the presence of carbon atoms in the alkyl chain of and the other peaks at 285.86 eV, and 287.06 eV with a shift of -0.8 eV & +2.1 eV may be due to the presence of impure carbon. The O 1s peak at 532 eV with a shift of +1 eV can be due to the adsorption of oxygen at the initial stages. The N 1s peaks at 399.00 eV and at 400.51 eV with the shift from the elemental binding energy of nitrogen at 398 eV, confirms the presence of nitrogen in the complex and S 2p peaks at 168.8 eV and 170.4 eV of 2p_{3/2} and 2p_{1/2} with the shift of +4.8 eV & +6.4 eV, with a separation of 0.6 eV, explains the presence of sulphur at different chemical situations and confirm the presence of thiolates on copper surface, where sulphur in the inhibitor molecule is being bonded with copper and the peak is due to the presence of Cu₂S. The absence of shake-up satellite peaks in the spectrum confirms the absence of Cu (II) species of copper which is due to the formation of thick SAMs and the SAMs formed might be sandwiched between the copper oxides, which prevent the further penetration and oxidation. Thus the shift in the elemental binding energies of N 1s and S 2p reveal that nitrogen and sulphur atoms present in azepane-1-carbo dithioic acid are involved in the complex formation through chelation with copper through cuprous ions. And the formation of thick inhibitor film due to the formation of SAMs is in agreement with SEM observations.

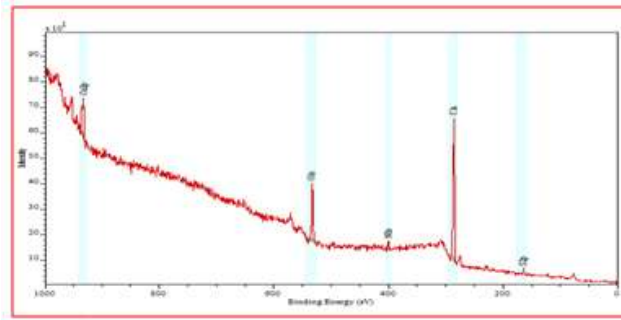


Fig. 5.1.1.a.

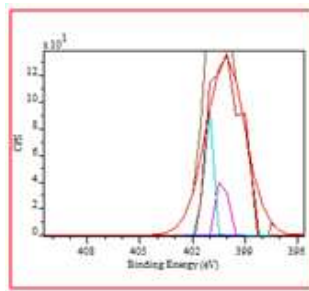


Fig. 5.1.1.b.

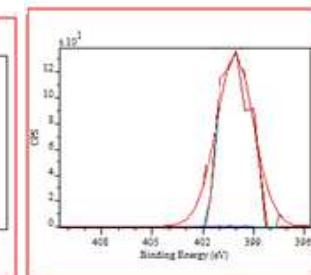
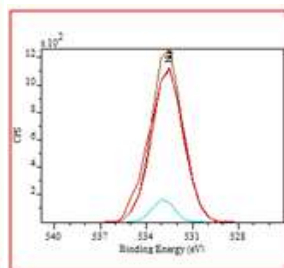


Fig. 5.1.1.c.

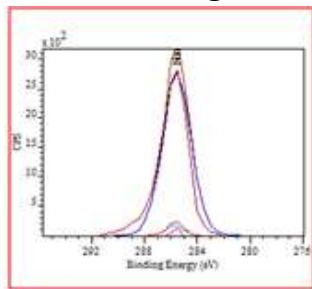


Fig. 5.1.1.d.

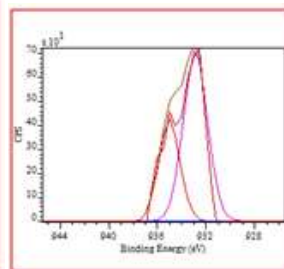


Fig. 5.1.1.e.

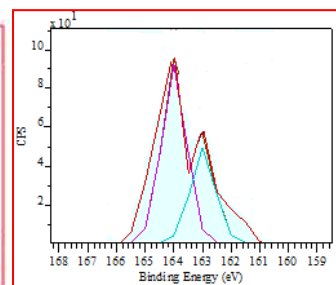


Fig. 5.1.1.f.

Figures 5.1.1. a, b, c, d, e, f represent the XPS survey spectrum and computer deconvoluted spectra of N 1s, C 1s, O 1s, Cu 2p, S 2p of SAMs covered copper respectively

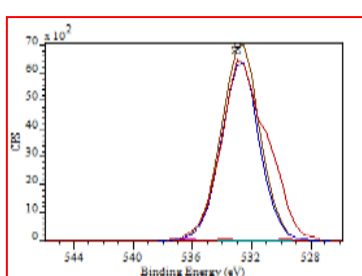


Fig. 5.1.2.a.

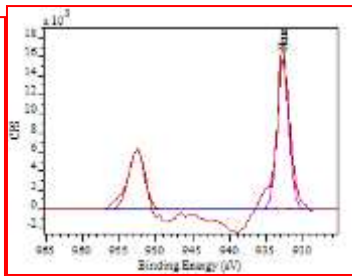


Fig. 5.1.2.b.

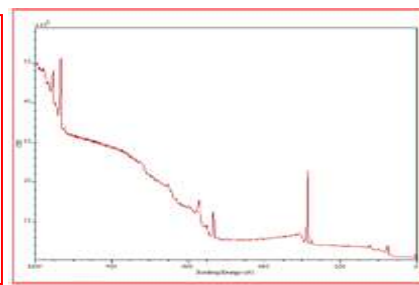


Fig. 5.1.2.c.

Figures 5.1.2. a, b, c represent the XPS survey spectrum and computer deconvoluted spectra of O 1s, Cu 2p of polished copper respectively

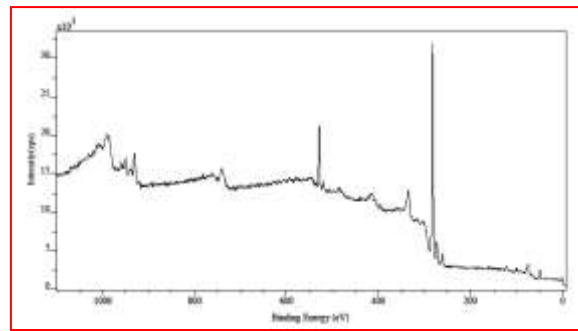


Fig. 5.1.3.a.

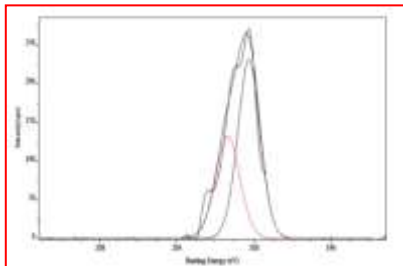


Fig. 5.1.3.b.

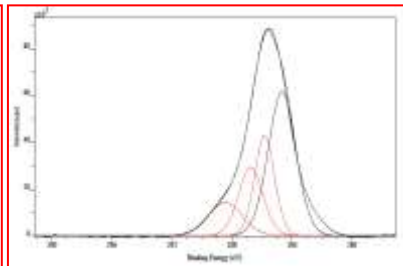


Fig. 5.1.3.c.

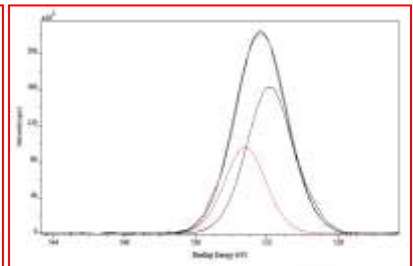


Fig. 5.1.3.d.

Figures 5.1.3. a, b, c, d represent the XPS survey spectrum and computer deconvoluted spectra of Cl 2p, C 1s, O 1s of copper in 300 ppm aq.sodium chloride respectively

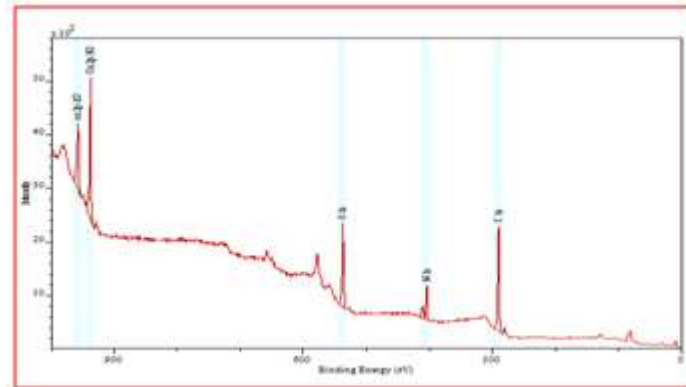


Fig. 5.1.4.a.

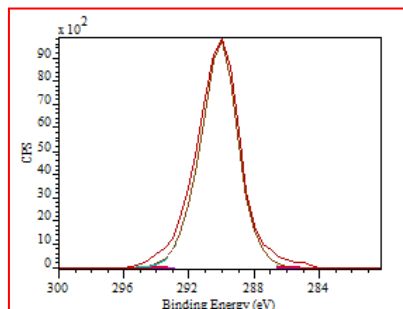


Fig. 5.1.4.b.

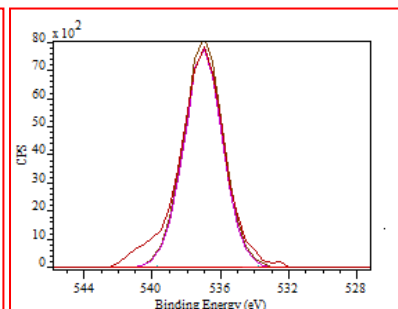


Fig. 5.1.4.c.

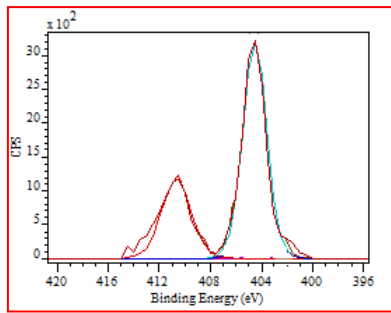


Fig. 5.1.4.d.

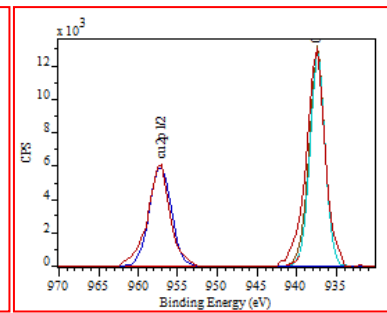


Fig. 5.1.4.e.

Figures 5.1.18.a, b, c, d, e represent the XPS survey spectrum and computer deconvoluted spectra of C 1s, O 1s, N 1s, Cu 2p, of SAMs covered copper respectively

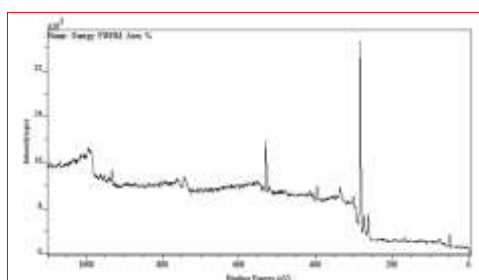


Fig. 5.1.5.a.

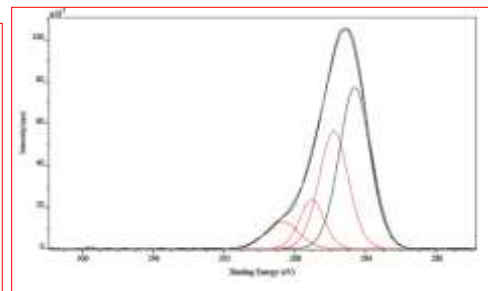


Fig. 5.1.5.b.

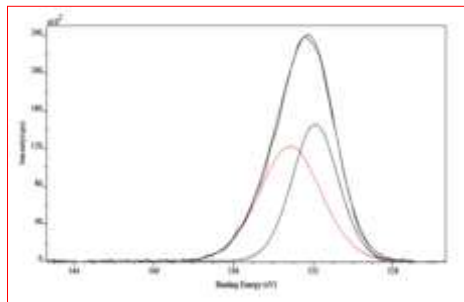


Fig. 5.1.5.c.

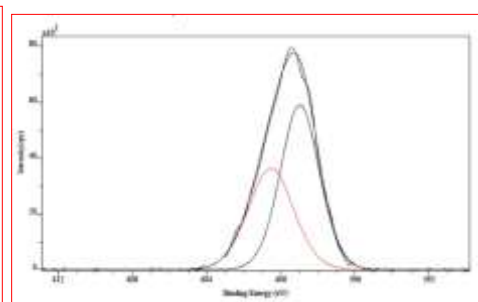


Fig. 5.1.5.d.

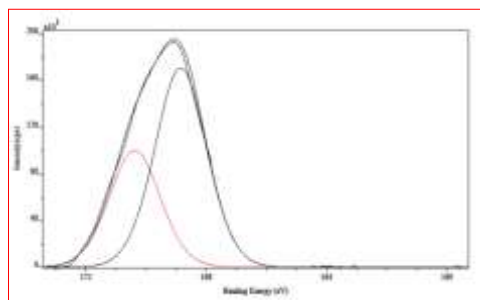


Fig. 5.1.5.e.

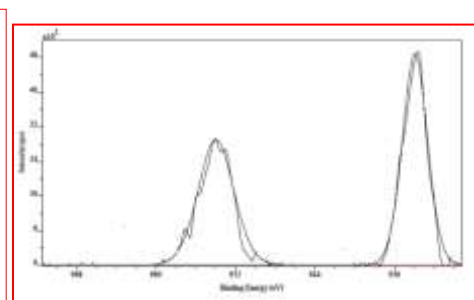


Fig. 5.1.5.f.

Figures 6.1.18.a, b, c, d, e, f represent the XPS survey spectrum and computer deconvoluted spectra of C 1s, O 1s, N 1s, S 2p, Cu 2p of SAMs covered copper respectively

6. Conclusion

Therefore it can be concluded that under these optimum conditions, i) polishing to mirror finish using 1-6 emery grade sheets, ii) degreasing with acetone, iii) ethanol and triple distilled water as solvent, the Self-assembled layers of thiol of 5 ppm, imidazole of 10 ppm and the amino acid of 20 ppm concentrations offer excellent protection to copper in neutral environment of various concentrations

from 100 to 300 ppm and in various immersion periods without much variation in the inhibition efficiencies. It is confirmed that among the thiol, imidazole and the amino acid used, thiol monolayer (5-methyl-1,3,4-thiadiazole-2-thiol) offers excellent inhibition efficiency upto 99% in protecting copper from corrosive environment such as in various sodium chloride concentrations and with various immersion periods. It is also further confirmed using surface characterization techniques.

References

1. Z. Quan, X. Wu, S. Chen, S. Zhao, H. Ma, *Corrosion* 57 (2001) 195.
2. Miki Ishibashi, Miki Itoh, Kiroshi Nishihara, Kunnitsugu Aramaki, *Electrochim. Acta* 41 (1996) 241.
3. Yang W, Gooding J J & Hibbert D B, *J Electroanal Chem*, 516 (2001) 10.
4. Myung M Sung & Kim Bull *Korean Chem. Soc.* 2001 Vol 22 No. 7
5. Ulman. A *An introduction to Ultrathin Organic films* Academic Press: Boston M A, 1991.
6. Laibins P.E., Whitesides G M, *J Am Chem Soc.* 1992, 114, 9022.
7. Guangzeng Liu, Xiuyu Liu, *J. Serb. Chem. Soc.* 73(5) 475-478 (2007) JSCS-3579.
8. S.S. Pathak, A.S. Khanna, *Indian Journal of Chem. Tech.*, Vol.14 Jan.2007 pp. 5-15.
9. Ulman A. *Chem Rev.* 96 (1996) 1533.
10. Laibins P. E. & Whitesides *J Am Chem Soc*, 117(1995) 12009.
11. Nuzzo R G & Allara D C, *J Am Chem Soc*, 105 (1983) 4481.
12. Maege I, Jaehne E, Henke A, Alder H J P, Bram C, Jung C & Stratmann M, *Prog Org Coat*, 34 (1998) 1.
13. Ishibashi M, Iton M, Nishihara H & Aramaki K, *Electrochim Acta*, 41 (1996) 241.
14. Jennings G K & Laibinis P E, *Colloids and Surfaces A-Physicochemical and Engineering Aspects*, 116 (1996) 105.
15. Jennings G K, Munro J C, Yong T S & Laibinis P E, *Langmuir*, 14 (1998) 6130.
16. Zamborini F G, Campbell J K & Crooks R M, *Langmuir* (1998) 640.
17. A.K. Satapathy, G. Gunasekaran, S.C. Sahoo, K. Amit, P.V. Rodrigues, *Corros. Sci*, 51 (2009) 2848.
18. B.V. Appa Rao, M. Narasihma Reddy, *J. Chem. Sci.* Vol. 125 Nov. 2013, pp. 1325-1338.